Environmental Science & Technology Letters

Letter

Cite This: Environ. Sci. Technol. Lett. 2018, 5, 209−213

pubs.acs.org/journal/estlcu

Imaging Organic−Mineral Aggregates Formed by Fe(II)-Oxidizing Bacteria Using Helium Ion Microscopy

James M. Byrne,*[,†] Matthias Schmidt,[‡] Tina Gauger,[†] Casey Bryce,[†] and Andreas Kappler[†]

[†]Center for Applied Geoscience, Geomicrobiology, University of Tuebingen, Sigwartstrasse 10, 72076 Tuebingen, Germany

[‡]Department of Isotope Biogeochemistry, ProVIS − Centre for Chemical Microscopy, Helmholtz Centre for Environmental Research GmbH − UFZ, Permoserstrasse 15, 04318 Leipzig, Germany

Supporting Information

ABSTRACT: Helium ion microscopy (HIM) has been used to image the development of mineralized twisted stalks produced by a neutrophilic, microaerophilic Fe(II)-oxidizing bacteria of the class *Zetaproteobacteria*. HIM is a relatively new type of microscopy which has several advantages over conventional scanning electron microscopy (SEM) due to its higher spatial resolution and the fact that samples can be imaged without coating (e.g., with Pt/Au). Here, we use HIM to show the development of nanometer- and micrometer-sized twisted stalk features consisting of organic material and Fe(III) minerals which appear to be loosely bound to the bacterial cells. These appendages are thought to be essential for eliminating Fe(III) waste produced during Fe(II) oxidation by sorbing Fe(III) and transporting it away from the cell. The results show the initial formation of long, precipitate-free stalks. After just 2 days, these became encrusted with spiky lepidocrocite crystals, and by 1 month, the characteristic twisted shape was almost indiscernible. These results demonstrate the high quality of images which can be obtained with helium ion microscopy from organic and mineral structures produced by bacteria without the requirement to sputter coat samples with conductive metals and can thus be considered to be more representive of how these structures would exist in the environment.

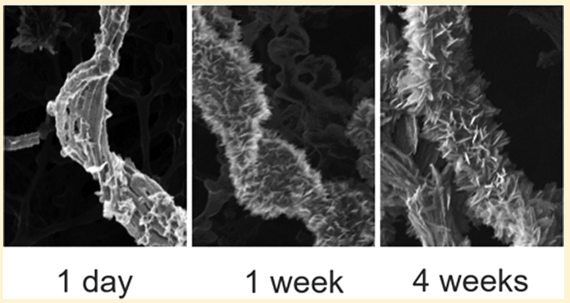

INTRODUCTION

Electron microscopy has long been used for studying biological materials such as bacteria at high resolution.[1] Transmission electron microscopy (TEM) provides high-resolution information on intracellular organelles but is restricted to very thin samples (<10s nm). Scanning electron microscopy (SEM) is more commonly used to study surface features of bacteria or minerals. There are, however, challenges associated with SEM, including limited resolution at high magnifications and the requirement to coat nonconductive materials (e.g., biological materials) with conductive metals such as platinum or gold. The use of such coatings has been shown to induce localized deposition of the metals in areas such as iron mineral structures rather than organic surfaces.[2] This local deposition can lead to artifacts, such as rough structures, which can be misinterpreted as being from the material under investigation. Helium ion microscopy (HIM) is a relatively new technique which can overcome many disadvantages of SEM. In HIM, helium ions (He^+) are focused into a smaller probe size with much smaller interaction volume at the sample surface compared to electrons. This leads HIM to have better material contrast and depth of focus compared to SEM. Furthermore, HIMs are equipped with charge compensation devices (flood gun) which enable imaging of nonconductive samples (such as organic material) without the requirement of sputter coating. In comparison, SEMs overcome charging by injection of nitrogen gas or water vapor, but this can lead to poor resolution and high background noise.[3] HIM can thus provide unparalleled resolution and contrast compared to SEM. In fact, it is estimated that the resolution of HIM is five times greater than that available with field emission SEM,[4] with 2−5 secondary electrons emitted per He ion.[4] One big disadvantage of HIM compared to SEM is the often lack of analytical detectors such as energy dispersive X-ray microscopy (EDX). Correlative microscopy enables the combination of such analytical tools available on an SEM with high resolution, high material contrast imaging available with HIM.

Despite such promising applications of HIM, the use of the technique for investigating biological samples is relatively sparse in the literature due to the limited availability of such instruments. The investigation of iron(Fe)-metabolizing bacteria is one potentially important application of HIM due to the presence of both organic structures and crystalline Fe minerals. Different types of Fe(II)-oxidizing bacteria are known to exist,[5] including (i) phototrophic Fe(II)-oxidizers,[6] (ii) nitrate-reducing Fe(II)-oxidizers,[7] and (iii) microaerophilic Fe(II)-oxidizing bacteria; the latter live in environments with

Received: February 13, 2018
Revised: March 3, 2018
Accepted: March 5, 2018
Published: March 5, 2018

DOI: 10.1021/acs.estlett.8b00077
Environ. Sci. Technol. Lett. 2018, 5, 209−213

opposing oxygen and Fe(II) gradients and often produce enigmatic structures including sheaths or twisted stalks which consist of Fe(III) minerals complexed to organic polymers.[8,9] There have been numerous studies which have applied either TEM or SEM to investigate the minerals formed by these types of bacteria; however, in almost all cases, the samples have been sputter coated with conductive materials.[10−13] A recent study by Zeitvogel et al. applied HIM to investigate the nitrate-reducing Fe(II)-oxidizer *Acidovorax* sp. BoFeN1.[14] Their results indicated that the surface of bacteria coated with Pt appeared to be shriveled with a rounded appearance, a feature not observed by HIM. This was considered to be due to preferential accumulation of Pt (used as sputter material) at exposed edges and tips of the minerals due to charge effects. This effect is one reason why applying techniques, such as HIM, can potentially provide important information which cannot be obtained by conventional SEM.

Here, we have used HIM, combined with correlative elemental mapping using SEM-EDX to investigate the mineralization of twisted stalks produced by microaerophilic Fe(II)-oxidizing bacteria to demonstrate the potential applications of the technique for environmental sciences. In particular, we focus on a strain isolated from a marine sedimentary environment which belongs to the class *Zetaproteobacteria*.[15−17] Similar types of bacteria have been shown to excrete closely bound fibrils which contain nanometer-sized Fe(III) (oxyhydr)-oxide minerals, predominantly ferrihydrite.[9,18] Over time, these fibrils become populated with lepidocrocite crystals which appear to nucleate on the surface. We aimed to understand how these lepidocrocite crystals develop over time on the fibrils without the influence of surface coatings from sputter materials and show how HIM could be applied in such studies.

MATERIALS AND METHODS

Microaerophilic Fe(II)-oxidizing bacteria were cultured in Petri dishes (diameter 5 cm) containing 9 mL of artificial seawater medium and 0.4 g of zerovalent iron (Fe(0)) powder. Here, 1 mL of inoculum was added to each plate. Twelve plates were prepared and stacked on top of each other in an anoxic jar (Merck; Darmstadt, Germany) with a gas pack (Dickinson and Co.; NJ, USA). The gas pack removes oxygen to yield microoxic conditions (6−10% of atmosphere).[17] Samples were taken at 6 h, 12 h, 24 h, 72 h, 96 h, 1 week, 2 weeks, and 4 weeks after inoculation corresponding to samples labeled 6h, 12h, 24h, 72h, 96h, 1w, 2w and 4w, respectively. The full sample preparation and imaging pathway is outlined in Figure S1. At each sampling point, the anoxic jar was opened, a single Petri dish removed, and then the jar sealed again with a fresh gas pack inserted. For sampling the Petri dish, under oxic conditions, 50 μL of sample was extracted away from Fe(0), which was held in place from the bottom using a magnet, and added to 5 mL of ultrapure MQ H_2O. The sample was then passed through a filter (0.44 μm). No attempt to fix the bacteria (e.g., with glutaraldehyde) was made. The filter was placed directly onto an aluminum SEM stub which had a layer of carbon tape underneath. Samples were not sputter coated.

Imaging was performed with a Zeiss Orion NanoFab HIM (Carl Zeiss Microscopy, Peabody, MA)[2] in secondary electron detection mode in conjunction with the flood gun used for charge compensation. The Everhardt−Thornley detector was biased at 300 V, and the electron flooding was done after the scan of each line. To investigate elemental composition of the stalks, in particular, to obtain distribution maps for iron, EDX was performed using a Zeiss Merlin VP compact field-emission (FE) SEM (Carl Zeiss Microscopy GmbH, Oberkochen, Germany) equipped with a Bruker Quantax FlatQUAD (Bruker Nano GmbH, Berlin,.Germany) EDX detector. For that, subsequent to HIM imaging, the samples had to be sputter-coated with AuPd since complete charge compensation is not possible in an SEM. In order to benefit from both the high lateral resolution of the HIM and the analytical capabilities of the SEM-EDX, EDX maps were acquired correlatively on the same regions previously imaged by HIM. Images from HIM and FE-SEM as well as elemental maps from EDX were overlaid using Correlia, an ImageJ plugin for multimodal image registration developed at UFZ Leipzig.

RESULTS AND DISCUSSION

Figure 1 shows, side by side, micrographs obtained via HIM (uncoated) and FE-SEM (coated with AuPd). Although both

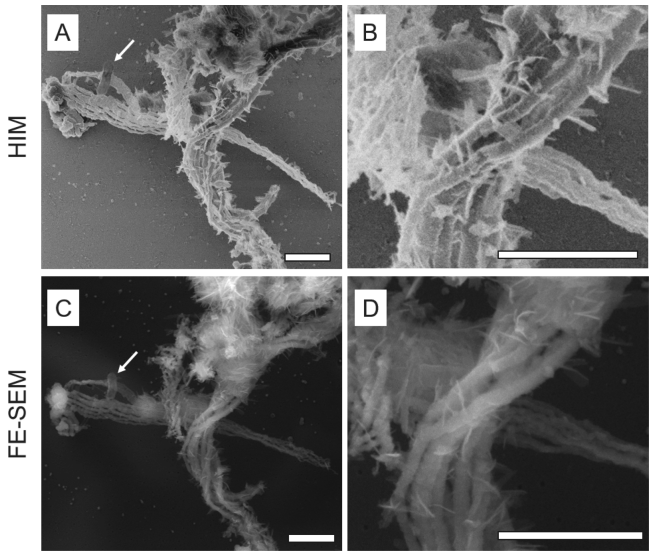

Figure 1. Micrographs of twisted stalks produced by microaerophilic Fe(II)-oxidizing bacteria. The figure shows a comparison between the results obtained using HIM (A and B) and FE-SEM (Acc. V = 12 kV, WD = 10 mm) (C and D). Scale bars are 1 μm. The arrow indicates a microaerophilic Fe(II)-oxidizing bacterial cell.

techniques use secondary electron detection for imaging and similar primary beam energies, the mechanisms of contrast formation are different. Helium ions generate secondary electrons of very low energies such that this type of microcopy is highly surface sensitive. Therefore, when imaging with HIM, edges are pronounced and slight charging of the sample manifests in darker regions in the image. On the contrary, secondary electrons generated by an electron beam exhibit much higher energies and can escape the sample even if generated several hundreds of nanometers below the surface depending on energy of the primary electrons or nature of the specimen. Furthermore, a strong material contrast stemming from inner shell secondary electron generation is obtained which makes heavier elements appear brighter than light elements. This is illustrated in Figure 1A and B. Both micrographs show comparatively similar results, with organic fibrous structures consisting of several parallel fibrils with an approximate thickness of 100 nm, loosely associated in a ribbon-like structure. These fibrils are characteristic of microaerophilic Fe(II)-oxidizing bacteria[17] and appear to be mostly

DOI: 10.1021/acs.estlett.8b00077
Environ. Sci. Technol. Lett. 2018, 5, 209−213

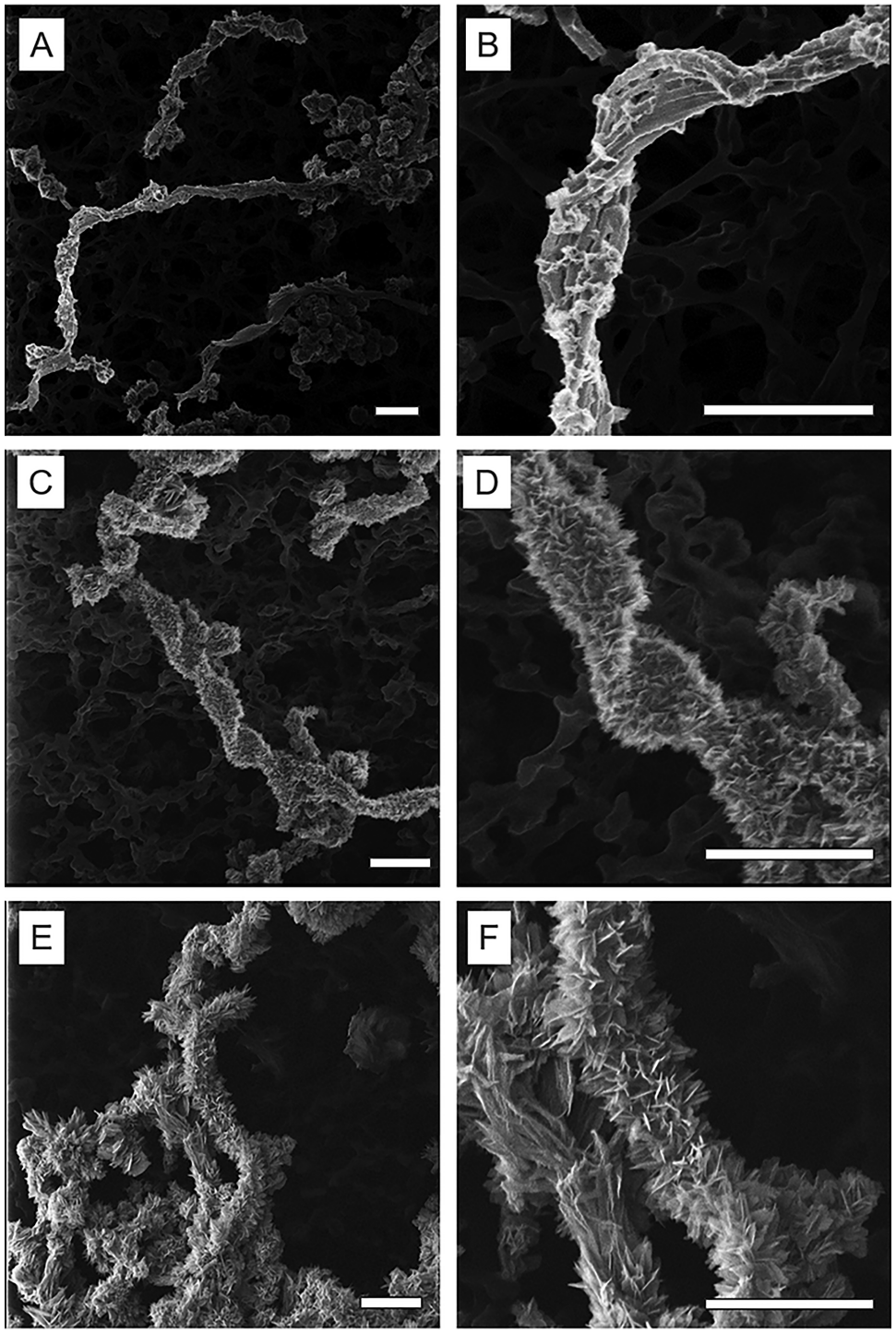

Figure 2. HIM micrographs of aged twisted stalks produced by microaerophilic Fe(II)-oxidizing bacteria. Samples were collected after (A,B) 24 h, (C,D) 96 h, and (E,F) 4 weeks. All scale bars are 2 μm.

smooth, with some small protruding features which are likely lepidocrocite crystals.[9] Large aggregates seen at the top of Figure 1A and B appear to be mineral aggregates which are potentially abiotic in origin. The difference in the surface sensitivity of HIM compared to FE-SEM can be seen for in Figure 1A which shows a well-defined object likely corresponding to a single bacterium on top of a stalk (see white arrow), while in Figure 1C, the same object appears to be semi-transparent. At higher magnification (Figure 1B and D), the HIM micrograph clearly shows finer features such as well-defined lepidocrocite crystals which are only visible as faint lines in FE-SEM. These lepidocrocite crystals typically form in a secondary mineralization process after the initial development of stalks.[9] Currently, however, it is unknown to what extent the formation of the crystals is due to enzymatic Fe(II) oxidation or abiotic oxidation of Fe(II) by O_2, in particular catalyzed by the stalk and/or mineral surface (heterogeneous oxidation). These results showed that HIM is able to yield more important information about the surface of an organic structure in comparison to FE-SEM, especially for uncoated samples. In

DOI: 10.1021/acs.estlett.8b00077
Environ. Sci. Technol. Lett. 2018, 5, 209−213

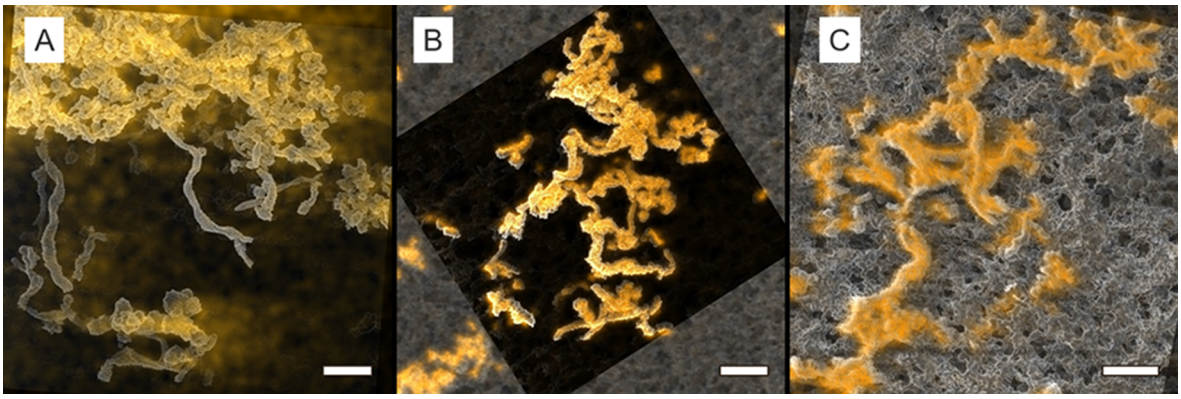

Figure 3. Correlative microscopy with EDX mapping corresponding to the Fe L edge (orange) overlaid onto HIM micrographs (A) 48 h, (B) 1 week, and (C) 2 weeks.

fact, investigation of uncoated samples is almost completely unachievable by SEM at such magnifications and in such quality.

To study the formation of crystalline features on twisted stalks produced by microaerophilic Fe(II)-oxidizers, a time series experiment was performed on new incubations. Samples were extracted at regular intervals and imaged using HIM (Figure 2). HIM was used to observe surface features in greater detail than achievable from FE-SEM. Images of samples collected after 6 h were dominated by spherical bulbous objects, which are presumably from the starting inoculum, or minerals formed by abiotic oxidation (Figure S2). For sample 24h, the signature twisted stalk features commonly associated with microaerophilic Fe(II)-oxidizing bacteria were evident (Figure 2A). The stalks consisted of several fibrils which were closely associated with one another. Each fibril had a thickness of ∼100 nm (Figure 2B). The HIM micrograph also revealed small precipitates on the fibers, while the background showed the presence of clusters of Fe(III) minerals which were presumably formed via abiotic oxidation. These results are in close agreement with those presented in Figure 1. With a larger field of view, it was possible to identify many twisted stalks which formed a spider web type of formation (Figure S3).

In sample 96h (Figure 2C), the formation of spiky minerals on the surface of the stalks were clearly evident, likely corresponding to lepidocrocite. This was confirmed with ^{57}Fe Mössbauer spectroscopy which indicated the presence of lepidocrocite and goethite in all samples (Figure S10, Table S1). The basic shape of the twisted stalk is still observable, although the needles completely surround the stalk (Figure 1D). As time increased, these spiky minerals became more prominent, suggesting mineral growth over time (Figures S2–S9). This is most easily observable for the 4 week old sample (4w) (Figure 2E and F) in which large crystals appear to have overgrown onto the twisted stalks fibers. In these images, it is still possible to identify the general shape of the twisted stalk; however, to an untrained observer, it could be easily overlooked that this structure was produced via biological activity.

Correlative microscopy was used to overcome the absence of analytical detectors on the HIM. Following the collection of images by HIM for samples 48h, 1w, and 2w, regions of interest (ROI) were mapped for each sample in relation to a reference mark on the sample holder. Several images were collected with progressively wider fields of view to make finding the ROI easier. In the FE-SEM, the ROI for each sample was located, and elemental mapping was performed. Using the ImageJ plugin Correlia, EDX elemental maps (in particular iron) were overlaid onto the HIM micrographs (Figure 3).

The results of elemental mapping suggested that sample 48h did not contain a high Fe content on the twisted stalks. In comparison, the globular structures, which we ascribe to be abiotic in origin, show a very high Fe signal. The 1w sample clearly showed a very bright signal corresponding to Fe on the twisted stalks, which persisted in sample 2w. These data suggest that initially the twisted stalks are not closely associated with iron, although a closer investigation of the HIM image for 48h clearly indicates the presence of spiky minerals on the surface of the stalks which likely correspond to lepidocrocite (Figure S4). It seems likely that in our case the counting time from EDX, which amounted to about 30 min and was limited by slow drift of the sample, was insufficient to observe the Fe present in the stalks with respect to the background material due to low Fe content. Nevertheless, the use of correlative imaging offers an opportunity to collect high resolution, high contrast micrographs using HIM while still retaining the ability to obtain analytical information.

We demonstrated here that helium ion microscopy is a powerful tool for observing mineral structures produced by bacteria. The high surface sensitivity and ability to image without the requirement of any coating (e.g., with Pt, Au, etc.) means that HIM can yield information without influence of artifacts created during the coating process. Therefore, with HIM, samples might actually appear as they are found in the environment. Furthermore, the high resolution means that the technique could provide greater information than normally available using FE-SEM. By applying correlative microscopy, we have shown that it is possible to combine the power of analytical methods available via SEM to obtain important information such as elemental distribution in such samples.

Our results show that twisted stalks produced by microaerophilic Fe(II)-oxidizers are initially produced without surface precipitates, but iron minerals quickly bind to the surface of the stalks. As time continues, these iron minerals become more and more mineralized, probably as a result of secondary, heterogeneous Fe(II) oxidation. The mechanisms behind the formation of twisted stalks by microaerophilic Fe(II)-oxidizing bacteria, and their function, remain points of debate. In particular, this includes whether the formation of the stalks is a simple response to Fe(II) toxicity? Or how much Fe(II) needs to be oxidized to produce enough electrons and ATP to synthesize all organics needed for the stalks? The use of HIM offers one potential approach to answering such open

DOI: 10.1021/acs.estlett.8b00077
Environ. Sci. Technol. Lett. 2018, 5, 209−213

questions. While the high resolution capabilities of HIM has been demonstrated, future applications of the instrument could focus on its nanofabrication capabilities which could make cross sectioning of twisted stalks possible to better understand the structural properties of the fibrils before, and after, mineralization by lepidocrocite surface crystals. Here, we have shown a new approach to study the growth of microaerophilic Fe(II)-oxidizing bacteria. Similar approaches could potentially be applied to obtain high resolution information on uncoated materials extracted from more complex environments such as in soils, sediments, biofilms, or materials collected from hydrothermal vents. Ultimately, we hope the outcome of this study will encourage environmental scientists to use HIM to support or improve imaging capabilities of materials containing both minerals and organics such as cell mineral aggregates which are ubiquitous in the environment.

■ ASSOCIATED CONTENT

Supporting Information

The Supporting Information is available free of charge on the ACS Publications website at DOI: 10.1021/acs.estlett.8b00077.

Detailed description of the measurement procedure for Mössbauer spectroscopy, schematic of sample preparation and imaging workflow (Figure S1), helium ion micrographs for samples collected between 6 h and 4 weeks (Figures S2–S9), and results from Mössbauer analysis (Figure S10 and Table S1). (PDF)

■ AUTHOR INFORMATION

Corresponding Author

*E-mail: james.byrne@uni-tuebingen.de.

ORCID

James M. Byrne: 0000-0002-4399-7336

Andreas Kappler: 0000-0002-3558-9500

Notes

The authors declare no competing financial interest.

■ ACKNOWLEDGMENTS

The authors are grateful for using the helium ion microscope at ProVIS – Centre for Chemical Microscopy at the Helmholtz Centre for Environmental Research, Leipzig, which is supported by European Regional Development Funds (EFRE – Europe funds Saxony) and the Helmholtz Association.

■ REFERENCES

(1) Miot, J.; Benzerara, K.; Kappler, A. Investigating microbe-mineral interactions: Recent advances in X-ray and electron microscopy and redox-sensitive methods. *Annu. Rev. Earth Planet. Sci.* **2014**, *42*, 271–289.

(2) Joens, M. S.; Huynh, C.; Kasuboski, J. M.; Ferranti, D.; Sigal, Y. J.; Zeitvogel, F.; Obst, M.; Burkhardt, C. J.; Curran, K. P.; Chalasani, S. H.; Stern, L. A.; Goetze, B.; Fitzpatrick, J. A. J. Helium Ion Microscopy (HIM) for the imaging of biological samples at sub-nanometer resolution. *Sci. Rep.* **2013**, *3*, 3514.

(3) Stokes, D. J.; Mugnier, J. Y.; Clarke, C. Static and dynamic experiments in cryo-electron microscopy: comparative observations using high-vacuum, low-voltage and low-vacuum SEM. *J. Microsc.* **2004**, *213*, 198–204.

(4) Ward, B.; Notte, J. A.; Economou, N. Helium ion microscope: A new tool for nanoscale microscopy and metrology. *Journal of Vacuum Science & Technology B: Microelectronics and Nanometer Structures Processing, Measurement, and Phenomena* **2006**, *24*, 2871–2874.

(5) Kappler, A.; Straub, K. L. Geomicrobiological Cycling of Iron. *Rev. Mineral. Geochem.* **2005**, *59*, 85–108.

(6) Jiao, Y.; Kappler, A.; Croal, L. R.; Newman, D. K. Isolation and Characterization of a Genetically Tractable Photoautotrophic Fe(II)-Oxidizing Bacterium, *Rhodopseudomonas palustris* Strain TIE-1. *Appl. Environ. Microbiol.* **2005**, *71*, 4487–4496.

(7) Larese-Casanova, P.; Haderlein, S. B.; Kappler, A. Biomineralization of lepidocrocite and goethite by nitrate-reducing Fe(II)-oxidizing bacteria: Effect of pH, bicarbonate, phosphate, and humic acids. *Geochim. Cosmochim. Acta* **2010**, *74*, 3721–3734.

(8) Emerson, D.; Fleming, E. J.; McBeth, J. M. Iron-oxidizing bacteria: an environmental and genomic perspective. *Annu. Rev. Microbiol.* **2010**, *64*, 561–583.

(9) Chan, C. S.; Fakra, S. C.; Emerson, D.; Fleming, E. J.; Edwards, K. J. Lithotrophic iron-oxidizing bacteria produce organic stalks to control mineral growth: implications for biosignature formation. *ISME J.* **2011**, *5*, 717–727.

(10) Schädler, S.; Burkhardt, C.; Hegler, F.; Straub, K.; Miot, J.; Benzerara, K.; Kappler, A. Formation of cell-iron-mineral aggregates by phototrophic and nitrate-reducing anaerobic Fe (II)-oxidizing bacteria. *Geomicrobiol. J.* **2009**, *26*, 93–103.

(11) Gauger, T.; Byrne, J. M.; Konhauser, K. O.; Obst, M.; Crowe, S.; Kappler, A. Influence of organics and silica on Fe (II) oxidation rates and cell–mineral aggregate formation by the green-sulfur Fe (II)-oxidizing bacterium Chlorobium ferrooxidans KoFox–Implications for Fe (II) oxidation in ancient oceans. *Earth Planet. Sci. Lett.* **2016**, *443*, 81–89.

(12) Laufer, K.; Nordhoff, M.; Røy, H.; Schmidt, C.; Behrens, S.; Jørgensen, B. B.; Kappler, A. Coexistence of microaerophilic, nitrate-reducing, and phototrophic Fe (II) oxidizers and Fe (III) reducers in coastal marine sediment. *Appl. Environ. Microbiol.* **2016**, *82*, 1433–1447.

(13) Klueglein, N.; Picardal, F.; Zedda, M.; Zwiener, C.; Kappler, A. Oxidation of Fe (II)-EDTA by nitrite and by two nitrate-reducing Fe (II)-oxidizing Acidovorax strains. *Geobiology* **2015**, *13*, 198–207.

(14) Zeitvogel, F.; Burkhardt, C. J.; Schroeppel, B.; Schmid, G.; Ingino, P.; Obst, M. Comparison of Preparation Methods of Bacterial Cell-Mineral Aggregates for SEM Imaging and Analysis Using the Model System of Acidovorax sp. BoFeN1. *Geomicrobiol. J.* **2017**, *34*, 317–327.

(15) McAllister, S. M.; Davis, R. E.; McBeth, J. M.; Tebo, B. M.; Emerson, D.; Moyer, C. L. Biodiversity and emerging biogeography of the neutrophilic iron-oxidizing Zetaproteobacteria. *Appl. Environ. Microbiol.* **2011**, *77*, 5445–5457.

(16) Scott, J. J.; Breier, J. A.; Luther, G. W., III; Emerson, D. Microbial iron mats at the Mid-Atlantic Ridge and evidence that Zetaproteobacteria may be restricted to iron-oxidizing marine systems. *PLoS One* **2015**, *10*, e0119284.

(17) Laufer, K.; Nordhoff, M.; Halama, M.; Martinez, R. E.; Obst, M.; Nowak, M.; Stryhanyuk, H.; Richnow, H. H.; Kappler, A. Microaerophilic Fe(II)-Oxidizing Zetaproteobacteria Isolated from Low-Fe Marine Coastal Sediments: Physiology and Composition of Their Twisted Stalks. *Appl. Environ. Microbiol.* **2017**, *83*, e03118-16.

(18) Toner, B. M.; Berquó, T. S.; Michel, F. M.; Sorensen, J. V.; Templeton, A. S.; Edwards, K. J. Mineralogy of iron microbial mats from Loihi Seamount. *Front. Microbiol.* **2012**, *3*, 1–18.

DOI: 10.1021/acs.estlett.8b00077
Environ. Sci. Technol. Lett. 2018, 5, 209–213